Characterization of Poly(*N*-isopropylacrylamide)-Grafted Interfaces with Sum-Frequency Generation Spectroscopy

Takayuki Miyamae,* Haruhisa Akiyama, Masaru Yoshida, and Nobuyuki Tamaoki

Nanotechnology Research Institute, National Institute of Advanced Industrial Science and Technology, 1-1-1 Higashi, Tsukuba 305-8565, Japan

Received February 15, 2007; Revised Manuscript Received March 30, 2007

ABSTRACT: Sum-frequency generation vibrational spectroscopy was used to study the molecular structure of surface-grafted poly(*N*-isopropylacrylamide) (PNIPAM) in air and in D_2O. It was found that the side chains of the PNIPAM were nearly standing at the air/PNIPAM interface, owing to the hydrophobic nature of the isopropyl groups. Total internal reflection geometry was employed to obtain SFG spectra of the D_2O/PNIPAM interface. When the water temperature was increased, red shifts of the SFG peaks were observed. This can be explained by the dehydration of the alkyl groups at the water interface. From the quantitative analysis of the molecular orientation, restructuring of the main chain due to the dehydration occurs at the water/PNIPAM interface is suggested.

Introduction

Thermoresponsive polymers may undergo soluble−insoluble transition when the temperature of the polymer solution is at the lower critical solution temperature (LCST). For example, poly(*N*-isopropylacrylamide) (PNIPAM) shows a phase separation at around 32 °C. PNIPAM has hydrophilic groups as well as hydrophobic groups, thus both hydrophilic and hydrophobic interactions are considered to be an important role in the thermoshrinking transition. This transition, when it occurs in solution, is referred to as a coil-to-globule transition and takes place over a narrow range of temperature. Recently, PNIPAM has received growing interest as an intelligent polymer in biotechnology,[1] because of its thermoresponsive function. When this polymer is grafted onto a solid substrate, the surface shows temperature-dependent properties, such as wettability and cell adhesion behavior.[2,3] The thermoresponsive surfaces have been successfully used to make a new system for the recovery of cells from tissue culture substrata without the need for proteolytic enzymes.[3]

The investigations of the phase transition behavior of the PNIPAM have mostly employed bulk polymer in aqueous solution.[4−6] However, the detailed study of the molecular structural informations at the water/PNIPAM interface are still limited. In this paper, we report infrared−visible sum-frequency generation vibrational spectroscopy (SFG) on the PNIPAM surface and water interface to study the thermally induced transition of the PNIPAM interfaces. Since SFG is a second-order nonlinear optical process, it is forbidden in media with inversion symmetry under the electric dipole approximation, but it is allowed where the inversion symmetry is broken.[7] A resonant enhancement in the SFG signal intensity is detected when the infrared beam frequency matches the molecular vibrational frequency. Because of its surface and interface sensitivity, SFG is a powerful tool for studying surfaces and interfaces. Recently, SFG has been applied to surface study,[8−10] the determination of the alignment of surface polymeric chains,[11−13] the study of the chemical composition of a surface, and for processing induced molecular structural changes at the interface.[14−16] Recently, Cheng and co-workers reported the use of the SFG and AFM techniques to probe the thermoresponsible behavior of the water/PNIPAM interface.[17] However, they have not tried to extract from the spectra detailed information about interfacial structures. We report here on the molecular restructuring behavior of the grafted-PNIPAM at water interfaces, with emphasis on extracting detailed information from the SFG measurements. The results indicate that the main chain of the PNIPAM reorients by increasing the water temperature. We also observe the hydration-induced blue-shifts of the SFG peaks at the water/PNIPAM interface.

* To whom correspondence should be addressed. Telephone: 81 29 861 4527: Fax: 81 29 861 6236. E-mail: t-miyamae@aist.go.jp.

Theory

Vibrational Sum Frequency Generation. In SFG, a pulsed visible beam ω_{VIS} and a pulsed tunable IR beam ω_{IR} are spatially and temporally overlapped on an area of the interface being probed. If the molecules at the interface are noncentrosymmetric, this overlapping results in the emission of a light at a sum frequency $\omega_{SF} = \omega_{VIS} + \omega_{IR}$.

The SFG experiments probe the nonlinear susceptibility $\chi^{(2)}$ and signal intensity can be expressed as $I \propto |\chi^{(2)}|^2$. The second-order nonlinear susceptibility $\chi^{(2)}$ represents a third-order tensor quantity which is described as the sum of non-resonant term $\chi_{NR}{}^{(2)}$ and a resonant term $\chi_R{}^{(2)}$. If the IR frequency is near vibrational resonance, $\chi^{(2)}$ can be written as

$$\chi^{(2)} = \chi_{NR}{}^{(2)} + \sum_q \frac{A_q}{\omega_{IR} - \omega_q + i\Gamma_q} \qquad (1)$$

where A_q, ω_q, and Γ_q are the strength, resonant frequency, and damping coefficient of vibrational mode q, respectively. The different components of the susceptibility tensor can be deduced by measuring the SFG spectra using different combinations of input and output beam polarizations. In this paper, SSP, SPS, and PPP are the three polarization combinations of interest, where S and P refer to light polarized in the plane of the interface and normal to the plane of interface, respectively. The polarization combination is abbreviated in the order such as SSP

10.1021/ma070399c CCC: $37.00
Published on Web 05/22/2007

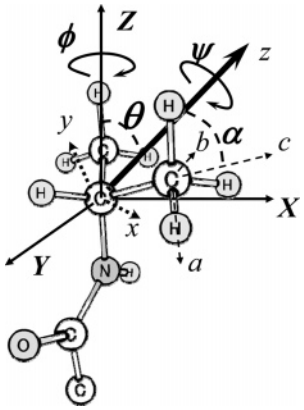

Figure 1. Geometry that defines the orientational angles, θ, ψ, and ϕ of the isopropyl groups of PNIPAM. The (a, b, c) axis is for methyl group fixed coordinates and (x, y, z) axis is for isopropyl fixed coordinates. The symbols θ, ψ, and ϕ represent the tilt angle, the twist angle about the z-axis, and the azimuthal angle about the Z-axis, respectively.

for S-polarized SFG, S-polarized visible, and P-polarized IR pulses. Expressions for the peak strengths of these polarization combinations are given as follows: [18]

$$A_{q,\mathrm{SSP}} = L_{YY}(\omega_{\mathrm{SF}})L_{YY}(\omega_{\mathrm{VIS}})L_{ZZ}(\omega_{\mathrm{IR}})\sin\Theta_{\mathrm{IR}}\chi_{XXZ} \quad (2)$$

$$A_{q,\mathrm{SPS}} = L_{YY}(\omega_{\mathrm{SF}})L_{ZZ}(\omega_{\mathrm{VIS}})L_{\mathrm{YY}}(\omega_{\mathrm{IR}})\sin\Theta_{\mathrm{VIS}}\chi_{YZY} \quad (3)$$

$$\begin{aligned} A_{q,\mathrm{PPP}} = {} & -L_{XX}(\omega_{\mathrm{SF}})L_{XX}(\omega_{\mathrm{VIS}})L_{ZZ}(\omega_{\mathrm{IR}})\cos\Theta_{\mathrm{SF}}\cos\Theta_{\mathrm{VIS}}\sin\Theta_{\mathrm{IR}}\chi_{XXZ} \\ & -L_{XX}(\omega_{\mathrm{SF}})L_{ZZ}(\omega_{\mathrm{VIS}})L_{\mathrm{XX}}(\omega_{\mathrm{IR}})\cos\Theta_{\mathrm{SF}}\sin\Theta_{\mathrm{VIS}}\cos\Theta_{\mathrm{IR}}\chi_{XZX} \\ & + L_{ZZ}(\omega_{\mathrm{SF}})L_{XX}(\omega_{\mathrm{VIS}})L_{\mathrm{XX}}(\omega_{\mathrm{IR}})\sin\Theta_{\mathrm{SF}}\cos\Theta_{\mathrm{VIS}}\cos\Theta_{\mathrm{IR}}\chi_{ZXX} \\ & + L_{ZZ}(\omega_{\mathrm{SF}})L_{ZZ}(\omega_{\mathrm{VIS}})L_{ZZ}(\omega_{\mathrm{IR}})\sin\Theta_{\mathrm{SF}}\sin\Theta_{\mathrm{VIS}}\sin\Theta_{\mathrm{IR}}\chi_{ZZZ} \end{aligned} \quad (4)$$

where Θ_{SF}, Θ_{VIS}, and Θ_{IR} are the reflection angles of the sum frequency, visible, and IR pulses, respectively. L_{ij} are Fresnel factors that describe the interfacial electric fields.

The orientation analysis of functional groups can be determined by using the oscillator strength A_q in eq 1. To perform the orientation analysis of the head groups of the side chain, we treat it to the similar manner as in the case of the SFG studies of leucine and 2-propanol.[19,20] The orientation of the isopropyl groups can be described by three angles, θ, ψ, and ϕ, as shown in Figure 1, when we use the coordinate system for the $-C(CH_3)_2$ groups (C_{2v} symmetry).[21,22] In this work, we assume the two methyl groups can rotate freely. Then, we found a_1 and b_1 vibrations for the symmetric stretch, and a_1, b_1, and b_2 vibrations for the asymmetric stretch. Here, the descriptions a and b denote the symmetric and the asymmetric modes with respect to the z-axis, and the subscripts 1 and 2 denote the in-plane and out-of-plane modes. Using this transformation, the hyperpolarizability tensor components β_{ijk} for the isopropyl group can be written in terms of the angle between two methyl groups 2α. For the symmetric stretch and the asymmetric stretch, β_{ijk} for the isopropyl group can be written as follows:

a_1 symmetric stretch

$$\begin{aligned} \beta_{xxz} &= -2(\beta_{aac} - \beta_{ccc})(\cos\alpha - \cos^3\alpha) + 2\beta_{aac}\cos\alpha \\ \beta_{yyz} &= 2\beta_{aac}\cos\alpha \\ \beta_{zzz} &= 2(\beta_{aac} - \beta_{ccc})(\cos\alpha - \cos^3\alpha) + 2\beta_{aac}\cos\alpha \end{aligned} \quad (5)$$

b_1 symmetric stretch

$$\begin{aligned} \beta_{zxx} &= -2(\beta_{aac} - \beta_{ccc})(\cos\alpha - \cos^3\alpha) \\ \beta_{xzx} &= -2(\beta_{aac} - \beta_{ccc})(\cos\alpha - \cos^3\alpha) \end{aligned} \quad (6)$$

a_1 asymmetric stretch

$$\begin{aligned} \beta_{xxz} &= -2\beta_{caa}(\cos\alpha - \cos^3\alpha) \\ \beta_{yyz} &= 0 \\ \beta_{zzz} &= 2\beta_{caa}(\cos\alpha - \cos^3\alpha) \end{aligned} \quad (7)$$

b_1 asymmetric stretch

$$\begin{aligned} \beta_{zxx} &= -\beta_{caa}(\cos\alpha - 2\cos^3\alpha) \\ \beta_{xzx} &= -\beta_{caa}(\cos\alpha - 2\cos^3\alpha) \end{aligned} \quad (8)$$

b_2 asymmetric stretch

$$\begin{aligned} \beta_{zyy} &= \beta_{caa}\cos\alpha \\ \beta_{yzy} &= \beta_{caa}\cos\alpha \end{aligned} \quad (9)$$

In this work, the bond angle between two methyl groups is assumed to be fixed at 110°.

Next, we have to transform all β_{ijk}s to the laboratory coordinate (X, Y, Z) system. In this experiment, PNIPAM surface is azimuthally isotropic, therefore, ϕ is uniformly distributed from 0 to 2π. Then, only 7 out of 27 components of the macroscopic hyperpolarizabilities $\chi_{IJK}^{(2)}$ are nonvanishing and only 4 are independent, namely, χ_{ZZZ}, $\chi_{XXZ} = \chi_{YYZ}$, $\chi_{XZX} = \chi_{YZY}$, and $\chi_{ZXX} = \chi_{ZYY}$. Then we have to transform the hyperpolarizability components β_{ijk} of isopropyl group fixed coordinates (x, y, z) to the laboratory coordinates (X, Y, Z). Each component in eqs 5−9 is substituted into the transformation table of ref 21 to obtain the relationship of the macroscopic hyperpolarizability tensor elements represented by (θ, ψ, ϕ), defined in Figure 1. The transformations are as follows.

Symmetric stretch:

a_1 vibration

$$\begin{aligned} \chi_{XZX} = \chi_{ZXX} &= (1/2)(\beta_{aac} - \beta_{ccc})[(\cos\alpha - \cos^3\alpha) \times \\ &\quad (3 + \cos 2\psi) - 2\cos\alpha](\cos\theta - \cos^3\theta) \\ \chi_{XXZ} = \chi_{YYZ} &= (1/2)(\beta_{aac} - \beta_{ccc})\{[(\cos\alpha - \cos^3\alpha) \times \\ &\quad (3 + \cos 2\psi) - 2\cos\alpha](\cos\theta - \cos^3\theta) - \\ &\quad 2(\cos\alpha - \cos^3\alpha)\cos\theta\} + 2\beta_{aac}\cos\alpha\cos\theta \\ \chi_{YZY} = \chi_{ZYY} &= (1/2)(\beta_{aac} - \beta_{ccc})[(\cos\alpha - \cos^3\alpha)(3 + \\ &\quad \cos 2\psi) - 2\cos\alpha](\cos\theta - \cos^3\theta) \\ \chi_{ZZZ} &= (1/2)(\beta_{aac} - \beta_{ccc})[(\cos\alpha - \cos^3\alpha)(1 + \cos 2\psi) \\ &\quad (\cos\theta - \cos^3\theta) + 2\cos^3\alpha\cos^3\theta] \end{aligned} \quad (10)$$

b_1 vibration

$$\chi_{XZX} = \chi_{ZXX} = -(\beta_{aac} - \beta_{ccc})(\cos\alpha - \cos^3\alpha) \times [\cos\theta - (\cos\theta - \cos^3\theta)(1 + \cos 2\psi)]$$

$$\chi_{XXZ} = \chi_{YYZ} = (\beta_{aac} - \beta_{ccc})(\cos\alpha - \cos^3\alpha) \times (\cos\theta - \cos^3\theta)(1 + \cos 2\psi)$$

$$\chi_{YZY} = \chi_{ZYY} = -(\beta_{aac} - \beta_{ccc})(\cos\alpha - \cos^3\alpha) \times [\cos\theta - (\cos\theta - \cos^3\theta)(1 + \cos 2\psi)]$$

$$\chi_{ZZZ} = -2(\beta_{aac} - \beta_{ccc})(\cos\alpha - \cos^3\alpha) \times (\cos\theta - \cos^3\theta)(1 + \cos 2\psi) \quad (11)$$

Asymmetric stretch:
a_1 vibration

$$\chi_{XZX} = \chi_{ZXX} = (1/2)\beta_{caa}(\cos\alpha - \cos^3\alpha) \times (\cos\theta - \cos^3\theta)(3 + \cos 2\psi)$$

$$\chi_{XXZ} = \chi_{YYZ} = -\beta_{caa}(\cos\alpha - \cos^3\alpha)[\cos\theta - (1/2) \times (\cos\theta - \cos^3\theta)(3 + \cos 2\psi)]$$

$$\chi_{YZY} = \chi_{ZYY} = (1/2)\beta_{caa}(\cos\alpha - \cos^3\alpha) \times (\cos\theta - \cos^3\theta)(3 + \cos 2\psi)$$

$$\chi_{ZZZ} = \beta_{caa}(\cos\alpha - \cos^3\alpha) \times [\cos\theta - 3\cos^3\theta + (\cos\theta - \cos^3\theta)\cos 2\psi] \quad (12)$$

b_1 vibration

$$\chi_{XZX} = \chi_{ZXX} = -(1/2)\beta_{caa}(\cos\alpha - 2\cos^3\alpha) \times [\cos\theta - (\cos\theta - \cos^3\theta)(1 + \cos 2\psi)]$$

$$\chi_{XXZ} = \chi_{YYZ} = (1/2)\beta_{caa}(\cos\alpha - 2\cos^3\alpha) \times [\cos\theta - (\cos\theta - \cos^3\theta)(1 + \cos 2\psi)]$$

$$\chi_{YZY} = \chi_{ZYY} = -(1/2)\beta_{caa}(\cos\alpha - 2\cos^3\alpha) \times [\cos\theta - (\cos\theta - \cos^3\theta)(1 + \cos 2\psi)]$$

$$\chi_{ZZZ} = -\beta_{caa}(\cos\alpha - 2\cos^3\alpha)(\cos\theta - \cos^3\theta) \times (1 + \cos 2\psi) \quad (13)$$

b_2 vibration

$$\chi_{XZX} = \chi_{ZXX} = (1/2)\beta_{caa}\cos\alpha[\cos\theta - (\cos\theta - \cos^3\theta)(1 - \cos 2\psi)]$$

$$\chi_{XXZ} = \chi_{YYZ} = -(1/2)\beta_{caa}\cos\alpha(\cos\theta - \cos^3\theta)(1 - \cos 2\psi)$$

$$\chi_{YZY} = \chi_{ZYY} = (1/2)\beta_{caa}\cos\alpha[\cos\theta - (\cos\theta - \cos^3\theta)(1 - \cos 2\psi)]$$

$$\chi_{ZZZ} = \beta_{caa}\cos\alpha(\cos\theta - \cos^3\theta)(1 - \cos 2\psi) \quad (14)$$

In these equations, we edited out the number density of the detected molecules N. From the SFG spectra, since the symmetric and the asymmetric CH_3 resonances are degenerate, we take the sum of these equations. Note, these equations include the angle α, but its value is assumed to be a constant. For simplicity, we shall assume δ-function distributions for both θ and ψ. In order to determine both θ and ψ, we have to assume the ratio of $R = \beta_{aac}/\beta_{ccc}$. It is known that R has to be in the range of about 1.66 to 4.0 for methyl group.[18,23] Thus, we assume $R = 2.1$, which is close to acetone ($R = 1.9$) and DMSO ($R = 2.3$).[24,25]

Experimental Section

Chemicals. All reagents, unless otherwise noted, were purchased from Wako Chemicals Japan, and were used without further purification. Anhydrous dichloromethane and anhydrous DMF were of organic synthesis grade, and others except acetone (>99%) were of special grade (>99.5%). NIPAM was purified by recrystallization from methanol twice. Aminopropyltriethoxysilane (APTES) was purchased from Shinetsu Silicone Chemicals, Japan.

Preparation of the Substrate and Grafted-PNIPAM. The IR grade fused quartz plates (Pier-Optics) were cleaned by sonication in acetone, ethanol containing 10 wt % KOH, and deionized water three times. Then the substrates were dried in vacuum for 1 h at room temperature. Amino group was introduced on the quartz surfaces by immersing the quartz plate into toluene solution of 1 wt % of APTES. The quartz plates were the rinsed with toluene and aged in an oven at 120° for 30 min. 2-Chloropropionyl chloride (0.15 g, 1.2 mmol), propionyl chloride (0.66 g, 7.1 mmol), and triethylamine (0.84 g, 8.3 mmol) were mixed in 20 mL of dichloromethane. The APTES treated quartz substrates were submerged in this solution for 2 h at room temperature. After being rinsed with ethanol, the substrates were immersed in the solution of 4 mL of DMF containing *N*-isopropylacrylamide (1.83 g, 16.2 mmol). The solution was purged with nitrogen flow, and then a 1 mL aqueous solution of CuCl (40 mg, 0.4 mmol) and tris[2-(dimethylamino)ethyl]amine (0.11 mL) was added to the DMF solution. After 2 h the fused quartz substrates were rinsed with methanol and dried under a stream of nitrogen. The IR grade fused quartz equatorial prism (Pier-Optics) was chemically modified with PNIPAM in a similar manner.

Contact Angle and FT-IR Measurement. Contact angles of water on the surfaces of PNIPAM grafted substrates were measured directly by video recording of a water droplet deposited on the substrates by using a precise temperature control stage. Transmission infrared measurements were carried out at a 4 cm^{-1} resolution using a Fourier transform IR spectrometer (Infinity, Mattson).

SFG Measurement. In IR-visible SFG experiments, a mode-locked Nd:YAG laser (PL2143D, EKSPLA) of 1064 nm with a pulse width of 20 ps and a repetition rate of 10 Hz was employed as a master light source. The detailed experimental setup has been described previously.[26] Briefly, a tunable IR beam was generated by an $AgGaS_2$ crystal by difference frequency mixing of the fundamental of the Nd:YAG laser with the output of an optical parametric oscillator/amplifier (OPO/OPA) system (PG401 VIR/DFG, EKSPLA). The OPO/OPA system employs a LiB_3O_5 crystal, which was pumped by the third harmonic of the Nd:YAG laser. The visible and IR beams were overlapped at a sample surface and their incidence angles were 70° and 50°, respectively. The pulse energy and the spot size of the tunable IR beam were 0.3 mJ and 0.5 mm (in diameter). The spectral resolution of the IR beam was 6 cm^{-1}. The SF output signal was filtered with a holographic notch filter and a monochromator (MS257, Oriel) and then detected by a photomultiplier tube (Hamamatsu, R649). Data were collected with 3 cm^{-1} increments in the region from 2750 to 3050 cm^{-1}, and the data were averaged over 200 laser shots. The SFG spectra were normalized for infrared and visible intensity variations.

In the case of the SFG measurements for water/PNIPAM interface, a geometry that almost enables total internal reflection of the green light was employed by using an equatorial fused quartz prism, as shown in Figure 2. The SFG output is enhanced by 1 to 2 orders of magnitude when the incidence angle of the input beam is close to the critical angle for total internal reflection.[27−29]

Results and Discussions

Characterization of the PNIPAM Grafted Surface. First, we characterized the PNIPAM grafted films by transmission FT-IR. Figure 3 shows the IR spectra of the film on the fused quartz and the spin-casted PNIPAM homopolymer film over

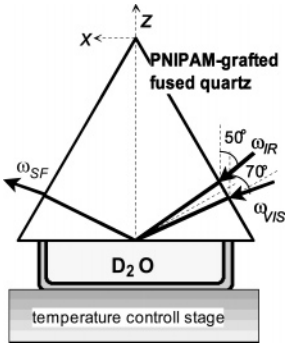

Figure 2. Schematic illustration of the experimental geometry of D_2O/PNIPAM interface.

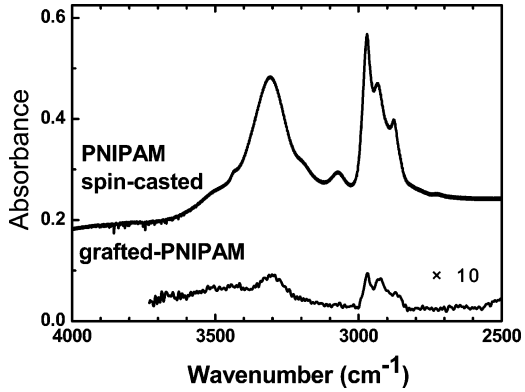

Figure 3. Transmission FT-IR spectra of the PNIPAM-grafted fused quartz and of the PNIPAM spin-casted film.

the range of 2500 to 4000 cm^{-1}. The IR spectrum of the grafted PNIPAM films is very similar to that of the PNIPAM homopolymer, and is almost identical with published results of PNIPAM films.[30,31] The peaks at 2970 and 2882 cm^{-1} are assigned to the antisymmetric and the symmetric CH stretch of the methyl groups, respectively.[30,31] The peak at 2939 cm^{-1} is due to the antisymmetric CH stretch of the methylene of the polymer backbone.[30] The broad feature around 3300 cm^{-1} is assigned to the NH stretch.

In order to evaluate the surface wettability of the grafted-PNIPAM, we measured water contact angle. At the substrate temperature of 14 °C, the water contact angle was about 53°, and it increased to 72° at 34 °C and 74° at 50 °C. Similar measurements taken on untreated fused quartz showed no change in the contact angles over the same temperature range. At room temperature, the PNIPAM swells in water to create a hydrophilic surface. Above LCST, the water is expelled, the polymer collapses, and the surface becomes less hydrophilic. Therefore, the surface wettability change with temperature confirms the thermoresponsive behavior of graft-PNIPAM.

PNIPAM Surface in Air. In Figure 4, we show the SFG spectra in the SSP, PPP, and SPS polarization combinations for the PNIPAM grafted on fused quartz substrate measured in air at room temperature. All the spectra are fitted by eq 1 with A_q, Γ_q, and ω_q that are allowed to vary to obtain best fits. The results are summarized in Table 1. The SSP SFG spectrum of the PNIPAM-grafted surface is almost identical to that of the PNIPAM spin-casted film in air (see Supporting Information). The peaks observed at 2871 and 2975 cm^{-1} are assigned to the symmetric and the asymmetric stretch of the CH_3 of isopropyl groups, respectively.[31] The peak at 2940 cm^{-1} may be derived from both the Fermi resonance of symmetric CH_3 and the methylene antisymmetric stretch.[31,32] The shoulder at around 2850 cm^{-1} is due to the symmetric stretch of the CH_2 group of

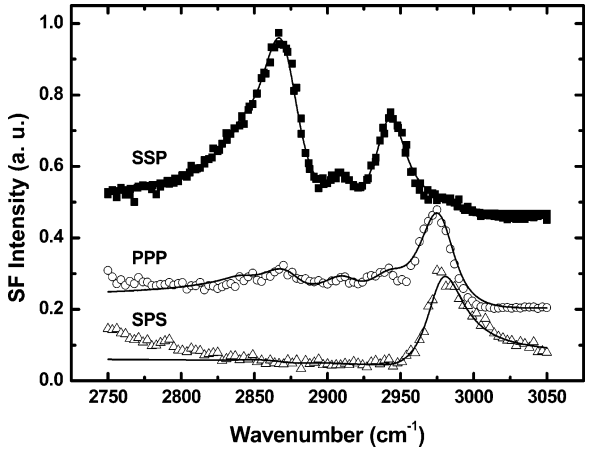

Figure 4. SSP, PPP, and SPS SFG spectra of the grafted-PNIPAM surface in air. The solid lines are the calculated fits to the data.

Table 1. Peak Assignments and the Parameters Computed from the Data Fitting of Figure 3

ω_q (cm^{-1})	Γ (cm^{-1})	A_{qSSP}	A_{qPPP}	A_{qSPS}	assignments	refs
2850	12	0.85	0.42	−0.02	*s*-CH_2	17, 20, 30−33
2871	16	7.95	2.16	−0.2	*s*-CH_3	17, 20, 30−33
2910	14	1.5	1.44	−0.1	CH	20, 33
2940	14	5.3	1.34	−0.3	*as*-CH_2 and *s*-CH_3 FR	17, 20
2975	14	1.1	6.5	−4.63	*as*-CH_3	17,20, 30−33

the main chain.[31,32] The weak SFG signal from the main chain must be due to the fact that the most of the PNIPAM surface is covered with the side chain. The small feature at 2910 cm^{-1} is assigned to the CH stretch of the methine group.[20,32] The observation of the strong CH_3 stretch peak together with the weak CH_2 peak indicates the presence of the ordered isopropyl groups tilting toward the surface normal in the ambient condition. Because of the hydrophobic property of the isopropyl end groups, the side chains tend to align in air with isopropyl groups pointing toward the air. A quantitative analysis of the peak strengths for the CH_3 can reveal the orientation of the isopropyl groups, as described in the theory section. In air atmosphere, the polar tilt angle θ of the isopropyl groups is about 40 ± 3°, with the twist angles ψ of about 10 ± 10°. This indicates that the side chains of the PNIPAM are nearly standing upright at the air/PNIPAM interface. Because of the hydrophobicity of the isopropyl termini, it is reasonable to think that the isopropyl groups are pointing toward the air.

Water—PNIPAM Interface. Total internal reflection (TIR) geometry was used to obtain SFG spectra of the water/PNIPAM interface. Because SFG depends on the local electric field, the signal from the interface is enhanced by proper selection of the incident angle and refractive index of the prism material. In view of the Fresnel enhancements due to the TIR of the visible light and the refractive index of PNIPAM (∼1.47),[34] SFG signals are almost exclusively produced at the water/PNIPAM interface. In Figure 5, we show the SFG spectra of D_2O/PNIPAM interface taken at the water temperatures of 20 and 50 °C. In both temperatures, thanks to the TIR geometry, we can obtain the SFG spectra with good resolution. The SFG intensities are slightly different for below and above LCST. We believe that the difference in intensities of the SFG signals is mainly caused by the disordering of the polymer chain owing to the high solubility of the PNIPAM at the temperature below LCST. From the SFG spectra, in addition to the signals derived from isopropyl groups, we can also observe the SFG peaks derived from the CH_2 groups of the main chain. Below LCST, the peaks observed at 2884 and 2985 cm^{-1} originate from the

Table 2. Parameters Computed from the Data Fitting of Figure 5

20 °C (<LCST)					50 °C (>LCST)					
ω_q	Γ	A_{qSSP}	A_{qPPP}	A_{qSPS}	ω_q	Γ	A_{qSSP}	A_{qPPP}	A_{qSPS}	assignments
2700	50	−11.0	27.6	5.0	2700	50	−14.0	43.5	16.8	−OD
2857	10	−0.55	0.69	−0.07	2857	10	−0.42	0.95	−0.16	*s*-CH_2
2884	10	−1.3	1.71	−0.15	2881	10	−0.99	2.1	−0.08	*s*-CH_3
2910	12	0.89	1.39	0.44	2903	12	0.60	1.3	0.49	CH
2934	12	−0.2	0.75	0.85	2927	12	−1.40	2.1	0.86	*as*-CH_2
2948	6	−0.79	1.0	−0.28	2948	6	−0.77	1.1	−0.15	*s*-CH_3 FR
2985	6	−0.08	1.4	−1.04	2975	6	−0.37	2.2	−2.12	*as*-CH_3
3180	180	−54.0	28.1	−1.5	3180	180	−56	29	−2.6	−OH

symmetric and the asymmetric stretch of the CH_3 of isopropyl groups, respectively. The peak at 2910 cm^{-1} is assigned to the CH stretch of the methine group. The peak at 2948 cm^{-1} is derived from the Fermi resonance of symmetric CH_3, which is much weaker in intensity than that in the air/PNIPAM interface. Since the Fermi resonance is assigned to the overtone bands of the CH_3 bending modes with the intensity borrowed from the methyl symmetric stretch band, it should be very sensitive to the interfacial structure.[35] The peaks at 2857 and 2934 cm^{-1} are due to the symmetric and the asymmetric stretch of the CH_2 group of the main chain, respectively. SFG resonance observed below 2800 cm^{-1} is caused by the OD stretch of D_2O (see Figure S3 of Supporting Information). We also observe the SFG signal above 3000 cm^{-1}, which must be caused by the OH stretch, which must be originated from the residual OH of the quartz interface. The intensity of the −OD resonance is significant increased by the elevating the temperature, possibly due to the change to the hydrophobic nature of the PNIPAM interface. Existence of the SFG peaks derived from the isopropyl groups at 20 °C indicates that the net orientational order of the hydrophobic termini is remained at the water/PNIPAM interface even below LCST. As seen, there is an abrupt shift of these bands toward lower frequencies upon heating. It should be noted that the peak shift caused by the heating in TIR geometry does not mean the changes in the refractive indices due to the reorientation of the PNIPAM at the water interface. The red-shift upon heating is also observed in the air-PNIPAM interface (see Supporting Information). IR experiments were suggested that the C−H stretching bands of alkyl groups undergo a blue shift when the alkyl group interacts with water.[32−38] The peak positions of the IR bands attributed to the symmetric (3 cm^{-1}) and the asymmetric CH_3 (10 cm^{-1}), CH (7 cm^{-1}), and the asymmetric CH_2 (7 cm^{-1}) show red-shifts upon heating. The blue shifts of the C−H stretching bands are in marked contrast to the red shift of an N−H and O−H stretching bands upon the formation of the hydrogen bond. In the C−H···OH_2 interaction, the exchange force is slightly larger than the forces for elongating of the hydrogen bonds. Therefore, below LCST, the hydrophobic isopropyl groups are interacting with surrounding water molecules. Above LCST, the red-shifts of the C−H bands are indicative of the dehydration of the alkyl groups at the water/PNIPAM interface.

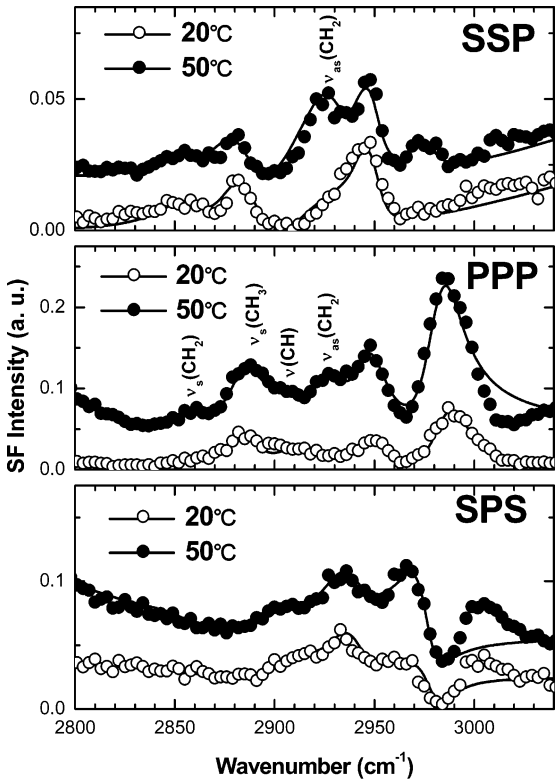

Figure 5. SSP, PPP, and SPS SFG spectra of the D_2O/PNIPAM interfaces. The solid lines are the calculated fits to the data.

Using the ratios of the fitted peak strengths, we can evaluate the values of θ and ψ at the water/PNIPAM interfaces. Below LCST, the orientational angles θ and ψ of the isopropyl groups are about 45 ± 5° and 15 ± 15°, respectively. Above LCST, θ is about 43 ± 3° and ψ, 10 ± 10°. The orientation of the isopropyl groups does not show significant differences in the angles for below and above LCST. It should be noticed that we assume the δ-function distribution for both θ and ψ in this analysis, because the surface coverage of isopropyl groups is unknown. This analysis does not mean the different orientational distribution of the isopropyl groups between below and above LCST.[39,40] We also examine the orientation of the main chain from the intensities of the symmetric and asymmetric CH_2 at PNIPAM/D_2O interfaces. From the quantitative analysis, we see the orientation of the main chain is drastically changes depending upon the water temperature. Below LCST, θ of the CH_2 is about 41°, and ψ, about 60°. On the other hand, above LCST, θ and ψ of the CH_2 are about 50° and 0°, respectively. The significant changes in the orientation angles of the main chain must be caused by the shrinking of the main chain due to dehydration. From the IR spectroscopic studies, it is reported that, below LCST, hydrated PNIPAM chains take a random coil configuration in an aqueous environment, and amide groups of PNIPAM are bound to water through a hydrogen-bond.[6,32] As the solution temperature increases, the intensity of the C═O···H_2O (D_2O) bonded peak is decreased, and instead, the formation of the C═O···N−H hydrogen-bond between neighboring amide groups along the polymer chain is accelerated.[32] That is, dehydration of the main chain leads to the contraction of intra- and interchain hydrogen-bonding, which induces the coil−globule transition. The formation of the intra- and interchain hydrogen-bonding would modify the orientation of the main chain. Therefore, we conclude that the restructuring of the main chain due to the dehydration occurs at the water/PNIPAM interface at the LCST of the PNIPAM.

Conclusions

We have studied the molecular structures of PNIPAM grafted on the fused quartz at air/PNIPAM and D_2O/PNIPAM interfaces. The polarization dependence of the peak intensities of the symmetric and asymmetric stretch of methyl groups were used to deduce the orientation of the side chain of the graft-PNIPAM interfaces. It was found that the side chains of the PNIPAM were nearly standing upright at air/NIPAM interface, owing to the hydrophobic nature of the isopropyl groups. At the PNIPAM/D_2O interface, the SFG signal intensities are changed depending on the water temperature, which is caused by the disordering of the polymer chain owing to the changes of the solubility of the PNIPAM. When the water temperature is increased, red-shifts of the SFG peaks due to the dehydration of the alkyl group are observed. This result indicates that the C−H groups interact with water below LCST. From the quantitative analysis of the molecular orientation, restructuring of the main chain due to the dehydration at the water/PNIPAM interface are suggested. This examination of the C−H stretch region by using SFG shows promising results in that we detect rearrangements of the PNIPAM grafted interface at the molecular level.

Acknowledgment. The authors thank Dr. Sho Kataoka for helpful discussions. This work is supported in part by Grant-in Aid for Scientific Research (No. 18550025).

Supporting Information Available: Figures showing the SFG spectrum in SSP polarization combination of the PNIPAM spin-casted film in air, substrate temperature-dependent SFG spectra of the PNIPAM in air, and the SFG spectrum in PPP polarization combination taken at the D_2O/PNIPAM interfaces from 2650 to 3050 cm^{-1}. This material is available free of charge via the Internet at http://pubs.acs.org.

References and Notes

(1) Huber, D. L.; Manginell, R. P.; Samara, M. A.; Kim, B. I.; Bunker, B. C. *Science* **2003**, *301*, 352−354.
(2) Ivanov, A. E.; Ekeroth, J.; Nilsson, L.; Mattiasson, B.; Bergenståhl, B.; Galaev, I. Y. *J. Colloid Interface Sci.* **2006**, *296*, 538−544.
(3) Yamada, N.; Okano, T.; Sakai, H.; Sakurai, Y. *J. Biomed. Mater. Res.* **1993**, *27*, 1243.
(4) Lin, S. Y.; Chen, K. S.; Run-Chu, L. *Polymer* **1999**, *40*, 2619−2624.
(5) Katsumoto, Y.; Tanaka, T.; Sato, H.; Ozaki, Y. *J. Phys. Chem. A.* **2002**, *106*, 3429−3435.
(6) Cheng, H.; Shen, L.; Wu, C. *Macromolecules* **2006**, *39*, 2325−2329.
(7) Shen, Y. R. *The Principles of Nonlinear Optics*; John Wiley & Sons: New York, 1984.
(8) Buck, M.; Himmelhaus, H. *J. Vac. Sci. Technol. A.* **2001**, *19*, 2717−2736.
(9) Wang, R. Y.; Himmelhaus, M.; Fick, J.; Herrwerth, S.; Eck, W.; Grunze, M. *J. Chem. Phys.* **2005**, *122*, Art. No. 164702.
(10) Lu, R.; Gan, W.; Wu, B. H.; Zhang, Z.; Guo, Y.; Wang, H. F. *J. Phys. Chem. B.* **2005**, *109*, 14118−14129.
(11) McGall, S. J.; Davies, P. B.; Neivandt, D. J. *J. Phys. Chem. B.* **2003**, *107*, 4718−4726.
(12) Clarke, M. L.; Wang, J.; Chen, Z. *Anal. Chem.* **2003**, *75*, 3275−3280.
(13) Miyamae, T.; Yokoyama, H.; Han, S.; Ishizone, T. *e-J. Surf. Sci. Nanotech.* **2006**, *4*, 515−520.
(14) Kweskin, S. J.; Komvopoulos, K.; Somorjai, G. A. *Langmuir*. **2005**, *21*, 3647−3652.
(15) Loch, C. L.; Ahn, D.; Chen, Z. *J. Phys. Chem. B.* **2006**, *110*, 914−918.
(16) Miyamae, T.; Nozoye, H. *Surf. Sci.* **2005**, *587*, 142−149.
(17) Cheng, X.; Canavan, H. E.; Stein, M. J.; Hull, J. R.; Kweskin, S. J.; Wagner, M. S.; Somorjai, G. A.; Castner, D. G.; Ratner, B. D. *Langmuir* **2005**, *21*, 7833−7841.
(18) Zhuang, X.; Miranda, P. B.; Kim, D.; Shen, Y. R. *Phys. Rev. B.* **1999**, *59*, 12632−12640.
(19) Ji, N.; Shen, Y. R. *J. Chem. Phys.* **2004**, *120*, 7107−7112.
(20) Kataoka, S.; Cremer, P. S. *J. Am. Chem. Soc.* **2006**, *128*, 5516−5522.
(21) C.; Akamatsu, N.; Domen, K. *Appl. Spectrosc.* **1992**, *46*, 1051−1072.
(22) Hirose, C. Unpublished results.
(23) Hirose, C.; Akamatsu, N.; Domen, K. *J. Chem. Phys.* **1992**, *96*, 997−1004.
(24) Yeh, Y. L.; Zhang, C.; Hermann, H.; Mebel, A. M.; Wei, X.; Lin, S. H.; Shen, Y. R. *J. Chem. Phys.* **2001**, *114*, 1837−1843.
(25) Allen, H. C.; Gragson, D. E.; Richmond, G. L. *J. Phys. Chem. B.* **1999**, *103*, 660−666.
(26) Miyamae, T.; Tsukagoshi, K.; Matsuoka, O.; Yamamoto, S.; Nozoye, H. *Langmuir* **2001**, *17*, 8125−8130.
(27) Beattie, D. A.; Haydock, S.; Bain, C. D. *Vib. Spectrosc.* **2000**, *24*, 109−123.
(28) Williams, C. T.; Yang, Y.; Bain, C. D. *Langmuir* **2000**, *16*, 2343−2350.
(29) Rangwalla, H.; Schwab, A. D.; Yurdumakan, B.; Yablon, D. G.; Yaganeh, S. H.; Dhinojwala, A. *Langmuir* **2004**, *20*, 8625−8633.
(30) Percot, A.; Zhu, X. X.; Lafleur, M. *J. Polym. Sci., Part B: Polym. Phys.* **2000**, *38*, 907−915.
(31) Maeda, Y.; Nakamura, T.; Ikeda, I. *Macromolcules* **2001**, *34*, 1391−1399.
(32) Maeda, Y.; Higuchi, T.; Ikeda, I. *Langmuir*. **2000**, *16*, 7503−7509.
(33) Maeda, Y.; Nakamura, T.; Ikeda, I. *Macromolecules* **2002**, *35*, 10172−10177.
(34) Francis, L. A; Friedt, J. M.; Zhou, C.; Bertrand, P. *Anal. Chem.* **2006**, *78*, 4200−4209.
(35) Gautam, K. S.; Dhinojwala, A. *Phys. Rev. Lett.* **2002**, *88*, 145501.
(36) Mizuno, K.; Ochi, T.; Shindo, Y. *J. Chem. Phys.* **1998**, *109*, 9502−9507.
(37) Gu, Y.; Kar, T.; Scheiner, S. *J. Am. Chem. Soc.* **1999**, *121*, 9411−9422.
(38) Katsumoto, Y.; Komatsu, H.; Ohno, K. *J. Am. Chem. Soc*. **2006**, *128*, 9278−9279.
(39) Wang, J.; Paszti, Z.; Mark, A.; Even, M. A.; Chen, Z. *J. Am. Chem. Soc.* **2002**, *124*, 7016−7023.
(40) Clarke, M. L.; Chen, C.; Wang, J.; Chen, Z. *Langmuir* **2006**, *22*, 8800−8806.

MA070399C